Towards measuring the ionisation and dissociation energies of molecular hydrogen with sub-MHz accuracy

Daniel Sprecher,[a] Christian Jungen,†[b] Wim Ubachs[c] and Frédéric Merkt*[a]

The most precise determination of the ionisation and dissociation energies of molecular hydrogen H_2 was carried out recently by measuring three intervals independently: the $X \rightarrow EF$ interval, the $EF \rightarrow n = 54p$ interval, and the electron binding energy of the $n = 54p$ Rydberg state. The values of the ionisation and dissociation energies obtained for H_2, and for HD and D_2 in similar measurements, are in agreement with the results of the latest *ab initio* calculations [Piszczatowski *et al.*, *J. Chem. Theory Comput.*, 2009, **5**, 3039; Pachucki and Komasa, *Phys. Chem. Chem. Phys.*, 2010, **12**, 9188] within the combined uncertainty limit of 30 MHz (0.001 cm^{-1}). We report on a new determination of the electron binding energies of H_2 Rydberg states with principal quantum numbers in the range $n = 51$–64 with a precision of better than 100 kHz using a combination of millimetre-wave spectroscopy and multichannel quantum-defect theory (MQDT). The positions of 33 np ($S = 0$) Rydberg states of *ortho*-H_2 relative to the position of the reference 51d ($N^+ = 1$, $N = 1$, $G^+ = \frac{1}{2}$, $G = 1$, $F = 0$) Rydberg state have been determined with a precision and accuracy of 50 kHz. By analysing these positions using MQDT, the electron binding energy of the reference state could be determined to be 42.3009108(14) cm^{-1}, which represents an improvement by a factor of $\sim$7 over the previous value obtained by Osterwalder *et al.* [*J. Chem. Phys.*, 2004, **121**, 11810]. Because the electron binding energy of the high-n Rydberg states will ultimately be the limiting factor in our method of determining the ionisation and dissociation energies of molecular hydrogen, this result opens up the possibility of carrying out a new determination of these quantities. By evaluating several schemes for the new measurement, the precision limit is estimated to be 50–100 kHz, approaching the fundamental limit for theoretical values of $\sim$10 kHz imposed by the current uncertainty of the proton-to-electron mass ratio.

I.   Introduction

H_2 (together with its deuterated isotopomers, HD and D_2) is the most fundamental molecular system that provides a quantitative understanding of chemical binding.

[a]Laboratorium für Physikalische Chemie, ETH-Zürich, 8093 Zürich, Switzerland. E-mail: feme@xuv.phys.chem.ethz.ch
[b]Laboratoire Aimé Cotton du CNRS, Université de Paris-Sud, 91405 Orsay, France
[c]Department of Physics and Astronomy, LaserLaB, VU University, De Boelelaan 1081, 1081 HV Amsterdam, The Netherlands

† Also at: Department of Physics and Astronomy, University College London, London, WC1E 6BT, UK.

Although it is only a four-particle system, molecular hydrogen is subject to all physical phenomena relevant to the description of chemical bonds in more complicated molecules. An accurate quantum-mechanical treatment of molecular hydrogen requires going beyond the Born–Oppenheimer approximation, and the inclusion of electron-correlation effects and of adiabatic, nonadiabatic, relativistic, and quantum-electrodynamical (QED) corrections.[1] The most common benchmark quantities used to test *ab initio* quantum-mechanical calculations of H_2 are the adiabatic ionisation energy E_i (the energy difference between H_2^+ in its rovibronic ground state with a free electron having no kinetic energy and H_2 in its rovibronic ground state) and the dissociation energy D_0 (the energy difference between two separated H atoms in the 1s state and H_2 in its rovibronic ground state).

Precise and accurate direct experimental measurements of ionisation and dissociation energies of molecules by spectroscopic methods are challenging because they necessitate either the determination of the onset of ionisation or dissociation continua in a spectrum, or the measurement of the kinetic energies of the fragments released following photoabsorption. Neither can be performed at the high-accuracy provided by currently available narrow-band laser sources. Typical experimental uncertainties of direct measurements of E_i and D_0 are in the order of 1 cm^{-1} and 10 cm^{-1}, respectively, although higher precision has been reached in favourable cases such as water[2] and molecular hydrogen.[3]

For E_i, more precise and accurate results are obtained if high-resolution spectra of highly excited Rydberg states are recorded and the Rydberg series extrapolated to their limits. This indirect method bypasses the necessity to localise the onset of the ionisation continuum and uses sharp transitions, the spectral positions of which can, in many cases, be determined with a precision and accuracy only limited by the linewidth of the transitions and the signal-to-noise ratio. The spectral position $\tilde{\nu}$ of a Rydberg state with principal quantum number n is approximately described by the Rydberg formula

$$\tilde{\nu} = \frac{E_i^{(\alpha^+)}}{hc} - \frac{R_M}{(n-\delta)^2}, \qquad (1)$$

where R_M is the mass-corrected Rydberg constant, δ is the quantum defect, and α^+ represents the quantum numbers needed to label the quantum state of the ion. However, extrapolation to the series limits using the Rydberg formula only yields accurate results if Rydberg states with $n > 100$ are used. In these cases, E_i can be determined with an accuracy of about 0.01 cm^{-1} (300 MHz).[4–6] Higher accuracies are in general not possible because of inevitable perturbations of the Rydberg series and systematic errors caused by stray electric fields.[7]

MQDT alleviates these limitations because it enables one to model the positions of Rydberg states with respect to the ionisation thresholds on the basis of a complete description of the channel interactions and parameters determined empirically or *ab initio*.[8,9] The present article illustrates, with the example of molecular hydrogen (H_2, HD and D_2), the power of the combination of high-resolution Rydberg spectroscopy with MQDT to determine E_i, and discusses its current limitations and future prospects. Because the ionisation and dissociation energies of H_2 are connected by the equation

$$D_0(H_2) = E_i(H_2) + E_i(H_2^+) - 2E_i(H) \qquad (2)$$

(and analogous equations for HD and D_2), which otherwise only contains the ionisation energies of one-electron systems, a measurement of $E_i(H_2)$ is also always a determination of $D_0(H_2)$. Indeed, $E_i(H_2^+)$ and $E_i(H)$ can be calculated with almost arbitrary precision and accuracy.[10,11] Consequently, molecular hydrogen represents one of the very few systems in which dissociation energies can be determined with a precision solely limited by the resolution of a spectroscopic experiment.

The evolution over the past 85 years of the recommended value of the dissociation energy of H_2 is summarised in Table 1. Consideration of this evolution leads to the conclusions that (1) enormous progress has been made in the determination of $D_0(H_2)$, both experimentally and theoretically; (2) precise experimental results have stimulated theoretical work and *vice versa*; (3) the evolution of the actual value has not been as smooth as the evolution of the uncertainties (see also Fig. 1); (4) a perfect agreement between theory and experiment at a given time does not imply a perfect agreement at later times. Not visible from the table, but obvious when

Table 1 The dissociation energy of H_2 as determined in selected earlier experimental and theoretical studies. The column denoted by Δ contains the determined value relative to the currently recommended dissociation energy of 36 118.06962(37) cm^{-1}.[12] All values are given in units of cm^{-1}

Year	Experiment	Theory	Δ	Ref.
1926	$35.2(19) \times 10^3$ [a]		-0.9×10^3	65
1927		24×10^3 [a,b]	-12×10^3	66, 67
1927	35.3×10^3 [a]		-0.8×10^3	68
1928		28.3×10^3 [a,b]	-7.8×10^3	69
1929	$36.19(32) \times 10^3$ [a]		0.07×10^3	70
1931		30.4×10^3 [a,b]	-5.7×10^3	71
1933		36 104(105) [a]	-14	72, 73
1934	36 100(40)		-18	74
1935	36 116(6)		-2	75
1960		36 113.1 [c]	-5.0	76
1961	36 113.05(30)		-5.02	77
1962		36 091	-27	78, 79
1964		36 114.2	-3.9	80
1966		36 117.5	-0.6	81
1968		36 117.4	-0.7	1
1969	36117.5(20) [d]		-0.6	82, 83
1969	36 118.3 [e]		0.2	84, 21
1970	36 118.6(5)		0.5	85
1972		36 117.8	-0.3	86
1975		36 118.0	-0.1	87
1978		36 117.92	-0.15	88
1983		36 118.01	-0.06	89
1986		36 118.088	0.018	90
1987		36 118.074	0.004	91
1992	36 118.11(8)		0.04	92, 93
1993	36 118.06(4)		-0.01	94
1993		36 118.049	-0.021	95
1993		36 118.060	-0.010	60
1995		36 118.069	-0.001	96
2004	36 118.062(10)		-0.008	3
2009	36 118.06962(37) [d]		0	12
2009		36 118.0695(10)	-0.0001	18

[a] For the conversion from eV to cm^{-1} the factor 8106 cm^{-1}/eV from Ref. 75 was used (the current value is 8065.54465(20) cm^{-1}/eV). [b] Corrected for a zero-point energy of 0.268 eV.[73] [c] Instead of the dissociation energy (D_0), a binding energy (D_e) of 4.7467 eV was given. To compare to experimental results, the value was converted to cm^{-1} (38 286.9 cm^{-1}), corrected for the experimental zero-point energy of 2179.3 cm^{-1}, and added to the adiabatic correction of 5.5 cm^{-1} (see Ref. 77 for details). [d] Determined from a measurement of the adiabatic ionisation energy using results of *ab initio* calculations on H_2^+ [see eqn (2)]. [e] Upper-bound value, which, according to Ref. 21, is more likely to be close to the true value than the lower-bound value 36 116.3 cm^{-1}.
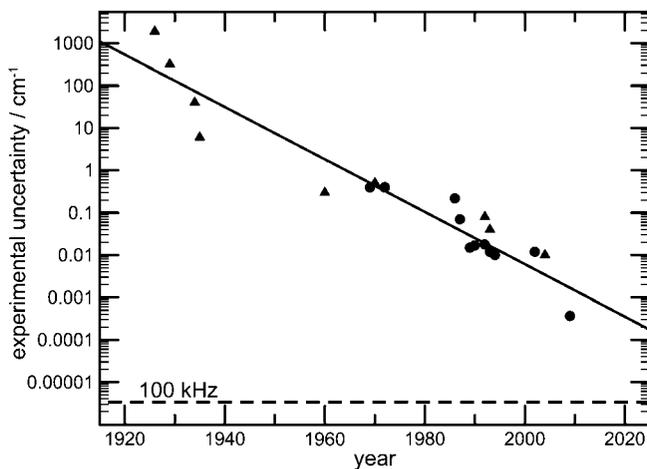
Fig. 1 Evolution of the experimental uncertainty of the adiabatic ionisation energy (circles) and the dissociation energy (triangles) of H_2. The values were taken from Table 1 of this article and Table III of Ref. 12. The solid line indicates the general trend that the experimental results gain an order of magnitude in accuracy every 14 years.

reading the corresponding references, is (5) the fact that the long-standing efforts invested to improve experimental and theoretical values of $D_0(H_2)$ have provided an exceptionally detailed and quantitative understanding of the different physical effects contributing to a chemical bond, including adiabatic, nonadiabatic, relativistic, and QED corrections to the Born–Oppenheimer approximation. As experiment and theory improve, unexpected effects and behavior may still be uncovered, and this alone provides a justification for further efforts.

The present article consists of four main parts. In the first (Section II), the latest measurements of E_i of molecular hydrogen are summarised and the results compared with the most recent calculations of this quantity. In the second part (Section III), we describe recent progress which has enabled us to determine the electron binding energies of high-n Rydberg states of H_2 with a precision of better than 100 kHz. In the third part (Section IV), we discuss possible ways to measure the energy of high-n Rydberg states with respect to the ground state and thus the ionisation and dissociation energies of molecular hydrogen with sub-MHz accuracy. In the fourth part (Section V), we discuss the current limits of purely *ab initio* MQDT and how these limits may be overcome in future.

II. Latest measurements of the ionisation energies of molecular hydrogen

The most recent measurements of the adiabatic ionisation energy of H_2 (Ref. 12), HD (Ref. 13), and D_2 (Ref. 14) have reached an accuracy of 11 MHz, 11 MHz, and 17 MHz, respectively ($\sim$0.0005 cm^{-1}). In all cases, the measurements relied on the determination of three energy intervals: the $X \rightarrow EF$ interval between the X electronic ground state and the $2s\sigma EF$ state, the $EF \rightarrow$ high-n interval between the EF state and a selected high-n Rydberg state (principal quantum number $n \approx 60$), and the high-$n \rightarrow X^+$ interval from the selected high-n Rydberg state to the onset of the ionisation continuum, corresponding to the X^+ ($v^+ = 0$, $N^+ = 0$) ground state of the H_2^+ ion. The measurements of these intervals were carried out independently and are briefly described in this section.

The $X \rightarrow EF$ interval was measured in a two-photon Doppler-free resonance-enhanced multiphoton ionisation (REMPI) experiment.[15] The fourth harmonic,

This journal is © The Royal Society of Chemistry 2011

around 202 nm, of the output of a pulsed titanium-doped sapphire (Ti:Sa) amplifier was used to excite the EF state in its vibrational ground state. The absolute frequency calibration was performed on the cw seed laser of the Ti:Sa amplifier using a frequency comb. The linewidth (full width at half maximum) of the observed two-photon transitions was less than 40 MHz and the transition frequencies could be determined with uncertainties in the range 3–6 MHz. The accuracy was limited by the frequency chirp induced by the pulse amplification and the residual Doppler shift resulting from a possible nonperfect overlap of the two counterpropagating laser beams. As an illustration of a typical measurement, Fig. 2 (a) shows the spectrum of the X ($v = 0$, $N = 1$) → EF ($v = 0$, $N = 1$) transition of H_2.[15]

The EF → high-n interval was measured by single-photon excitation using the second harmonic, around 400 nm, of the output of a pulse-amplified Ti:Sa laser.[12–14] The absolute transition frequencies were obtained by measuring the difference of the fundamental cw Ti:Sa laser frequency to the positions of selected iodine absorption lines which had themselves been calibrated using a frequency comb. The Doppler-limited linewidth in these experiments was ∼120 MHz and the intervals could be determined with uncertainties in the range 10–20 MHz. The accuracy was mainly limited by the Doppler width of the observed resonances and by Stark shifts of the final Rydberg states caused by residual stray electric fields in the excitation region. As an example of a measurement of the EF → high-n interval, the spectrum of the EF ($v = 0$, $N = 1$) → $54p1_1$ ($S = 0$) transition of H_2 is shown in Fig. 2 (b).[12] The notation $n\ell N_N^+$ is used to label Rydberg states throughout this article (all quantum numbers have their usual meanings, see, e.g., Table I in Ref. 16). All Rydberg states considered in this article converge to the X^+ ($v^+ = 0$) state of H_2^+, HD^+ or D_2^+, although higher rovibrationally excited states can also be used for an extrapolation of the ionisation energies.[13] Because the relative energies of the lowest rotational levels of both neutral and ionised species are known with high accuracy, E_i and D_0 can be derived from measurements of Rydberg series converging to excited rotational levels. In practice, Rydberg series converging to the lowest rotational levels ($N^+ = 0$ and 1) are most convenient because autoionisation does not lead to undesirable line broadening.
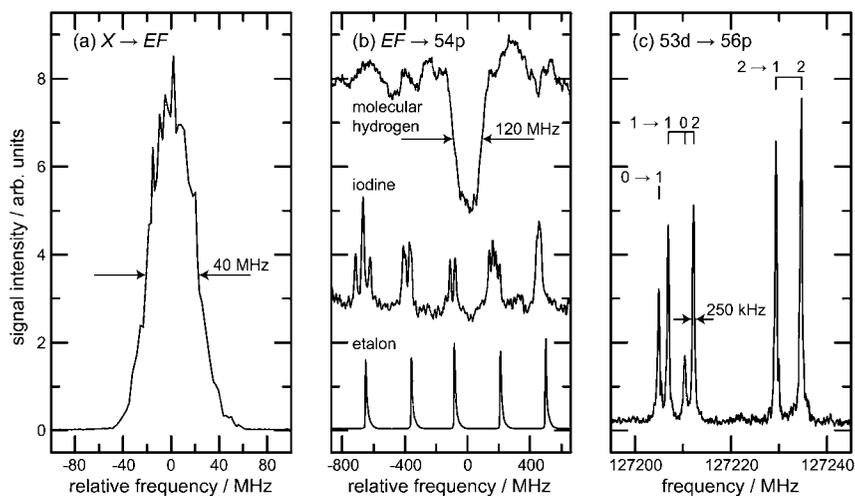
Fig. 2 Spectra showing (a) the X ($v = 0$, $N = 1$) → EF ($v = 0$, $N = 1$); (b) the EF ($v = 0$, $N = 1$) → $54p1_1$ ($S = 0$); (c) the $53d1_1$ ($G^+ = \frac{1}{2}$, $G = 1$) → $56p1_1$ ($S = 0$) transitions of *ortho*-H_2. For the measurement shown in panel (b) Doppler-free iodine spectra and etalon traces were recorded simultaneously and the spectra were shifted along the vertical axis for clarity. Above the assignment bars in panel (c), the total angular momentum quantum number F of the initial and final hyperfine states are given.

The high-$n \to X^+$ interval was determined using millimetre-wave spectroscopy of transitions between high-n Rydberg states in combination with multichannel quantum-defect theory (MQDT), including rovibrational channel interactions and hyperfine effects.[16] The relative energies of 68 np, 48 nd, and 86 nf Rydberg states of H_2 with n in the range 51–64 were determined with an accuracy of better than 1 MHz. The millimetre-wave spectrum of the $53d1_1$ ($G^+ = \frac{1}{2}$, $G = 1$) $\to 56p1_1$ ($S = 0$) transition is shown as an example in Fig. 2 (c). MQDT was used to determine the ionisation energies of the p and f states with an accuracy of 600 kHz and to extrapolate the hyperfine structure of H_2^+ in the X^+ ($v^+ = 0$, $N^+ = 1$) state. In a similar experiment on D_2, the hyperfine structure of D_2^+ in the X^+ ($v^+ = 0$, $N^+ = 1$) state could be determined and the main MQDT parameters (the eigenquantum defects; see Section III) were shown to be independent of isotopic substitution within the uncertainty limits of the determination (600 kHz).[17] The high-$n \to X^+$ interval could therefore be determined for H_2, HD, and D_2 with an accuracy of better than 1 MHz.

The experimental values of the adiabatic ionisation energies of H_2, HD, and D_2 are given in Table 2, where they are compared with the latest *ab initio* values of these quantities.[18,19] The present status of the comparison between experimental and theoretical determinations of E_i and D_0 is that experimental and theoretical results are in agreement within the combined uncertainties (0.001 cm^{-1} or 30 MHz) for all three isotopomers of molecular hydrogen. The experimental results can therefore be regarded as a validation of the *ab initio* calculations, and, together, experiment and theory enable one to quantify the different contributions to D_0 (see Table 2). The dissociation energy in the Born–Oppenheimer approximation, including the

Table 2 *Ab initio* values of the adiabatic ionisation energies of H_2, HD, and D_2 and the terms from which they were determined. Columns denoted by α^n contain the sum of the relativistic and QED corrections of order n in the fine-structure constant α. All values are given in units of cm^{-1}

	Nonrel. energy	α^2	α^3	α^4	α^5	Total	Ref.
Dissociation energies of H_2, HD, and D_2							
$D_0(H_2)$	36 118.7978[a]	−0.5319	−0.1948	−0.0016		36 118.0695(10)	18
$D_0(HD)$	36 406.5108[a]	−0.5300	−0.1964	−0.0016		36 405.7828(10)	19
$D_0(D_2)$	36 749.0910[a]	−0.5278	−0.1983	−0.0016		36 748.3633(9)	18
Adiabatic ionisation energies of H, D, H_2^+, HD$^+$, and D_2^+							
$E_i(H)$	109 677.58341	1.46091	−0.27076	−0.00194	0.00012	109 678.77174	11
$E_i(D)$	109 707.42659	1.46071	−0.27093	−0.00194	0.00012	109 708.61455	11
$E_i(H_2^+)$	131 056.87575	1.59950	−0.35093	−0.00249	0.00015	131 058.12198(6)	10
$E_i(HD^+)$	131 223.43626	1.60191	−0.35168	−0.00250	0.00015	131 224.68415(6)	10
$E_i(D_2^+)$	131 418.94771	1.6051	−0.35255	−0.00250	0.00015	131 420.1979(4)	14, 97, 98
Adiabatic ionisation energies of H_2, HD, and D_2							
$E_i(H_2)$[b]	124 417.0889	0.7904	−0.3854	−0.0030	0.0001[e]	124 417.4910(10)	
Experiment						124 417.49113(37)	12
$E_i(HD)$[c]	124 568.0845	0.7897	−0.3864	−0.0030	0.0001[e]	124 568.4849(10)	
Experiment						124 568.48581(36)	13
$E_i(D_2)$[d]	124 744.9965	0.7885	−0.3876	−0.0030	0.0001[e]	124 745.3945(9)	
Experiment						124 745.39407(58)	14

[a] The nonrelativistic contributions to the dissociation energies of H_2, HD, and D_2 consist of a dominant term corresponding to the Born–Oppenheimer approximation (36 112.5927 cm^{-1}, 36 401.9332 cm^{-1}, and 36 746.1623 cm^{-1}, respectively), an adiabatic correction (5.7711 cm^{-1}, 4.2509 cm^{-1}, and 2.7725 cm^{-1}, respectively), and a nonadiabatic correction (0.4339 cm^{-1}, 0.3267 cm^{-1}, and 0.1563 cm^{-1}, respectively).[18,19] [b] Determined using $E_i(H_2) = D_0(H_2) - E_i(H_2^+) + 2E_i(H)$. [c] Determined using $E_i(HD) = D_0(HD) - E_i(HD^+) + E_i(H) + E_i(D)$. [d] Determined using $E_i(D_2) = D_0(D_2) - E_i(D_2^+) + 2E_i(D)$. [e] Only contributions from the one-electron systems (H, D, H_2^+, HD$^+$, and D_2^+). No α^5 contribution has been calculated for H_2, HD, and D_2.

zero-point vibrational energy, represents the largest contribution (99.985% for H_2, 99.989% for HD, and 99.994% for D_2). The second largest contribution is the adiabatic correction, which, at first approximation, is inversely proportional to the reduced mass and accounts for 0.016%, 0.012%, and 0.0075% of D_0 in H_2, HD, and D_2, respectively. The nonadiabatic corrections also rapidly decrease with the mass and account for 1.2×10^{-3} % (H_2), 0.9×10^{-3} % (HD), and 0.4×10^{-3} % (D_2) of D_0. The relativistic α^2 (1.5×10^{-3} %) and the QED α^3 (0.5×10^{-3} %) corrections are essentially independent of isotopic substitution and have the opposite sign to the adiabatic and nonadiabatic corrections. The one-loop electron self-energy (QED) term is the dominating α^4 correction (see discussion in Ref. 18 and 20). It has been evaluated to be only 4.4×10^{-6} % of D_0 but needs to be included to reach agreement with the experimental results. The current uncertainty in the proton-to-electron mass ratio $\mu = m_p/m_e$ [$\delta\mu/\mu = 4.3 \times 10^{-8}$ % (Ref. 11)] is expected to only affect the value of D_0 at the level of 14 kHz (4.8×10^{-7} cm^{-1}, *i.e.* 1.3×10^{-9} %), as estimated by assuming that the zero-point vibrational energy is proportional to $\mu^{-\frac{1}{2}}$ (harmonic approximation).

III. Determination of the high-$n \rightarrow X^+$ interval by millimetre-wave spectroscopy and MQDT

The main advantage of the method of determining the ionisation and dissociation energies of molecular hydrogen presented in the previous sections is that it does not rely on the measurement of the onset of a continuum. Continua are intrinsically weak, their onsets are rarely observable as sharp steps and may be obscured by other spectral features or affected by stray electric fields.[21] The resulting ambiguities limit the precision and accuracy of the measurements. Measurements of the spectral positions of individual Rydberg states do not suffer from these ambiguities, but necessitate a reliable method to extract the Rydberg-electron binding energies.

The use of the Rydberg formula [eqn (1)] represents the simplest method. However, it corresponds to a single-channel treatment of photoionisation, and does not account for the interactions between the channels associated with the different vibrational, rotational, and hyperfine levels of the molecular ion to which the Rydberg series converge. Multichannel quantum-defect theory (MQDT) represents the method of choice because it enables a full treatment of the electron-ion scattering. However, the parameters used in actual calculations (*i.e.*, the energy level structure of the molecular ion, and the eigenquantum-defect functions which are dependent on both energy and internuclear distance) must either be known or adjusted to fit the experimental results to the desired accuracy.

The MQDT model we use to derive the electron binding energies of Rydberg states of H_2, HD, and D_2 has been presented in detail in Ref. 16. Starting values for the eigenquantum defects were obtained *ab initio* and refined by using a large set of relative energies of p and f Rydberg states of H_2 in the range $n = 54$–64 obtained by millimetre-wave spectroscopy [see Fig. 2(c)]. As explained in the previous section, the electron binding energies of these states could be determined in a global fit of 18 MQDT parameters using a total of 154 level positions with an absolute accuracy of 600 kHz. Several aspects of the analysis remained incomplete. First, the relative positions of p and f Rydberg levels were extracted from the millimetre-wave spectra by building combination differences starting from the lowest observed level [the 51d1$_1$ ($G^+ = \frac{1}{2}$, $G = 1$, $F = 0$) level] and systematically extending the network of level positions towards higher levels. The positions of the highest observed levels (with $n = 64$) were thus obtained as sums and differences of up to 15 measured transition frequencies, each contributing its own uncertainty. This led to less accurate energies and therefore lower statistical weights for the higher observed levels. Second, no fully satisfactory way could be devised to assess the Stark shifts of the f levels, which were consequently given conservative systematic

uncertainties, with unquantifiable consequences on the uncertainties of the electron binding energies determined in the MQDT fit. Finally, the accuracy limit of the frame-transformation approximation on which the MQDT calculations rely could not be firmly established, only its upper bound, *i.e.* 600 kHz, limited by the experimental uncertainties. Comparison with coupled-equation calculations suggested, however, that the frame-transformation approximation leads to significantly smaller errors.[16] Establishing an improved upper bound for the accuracy limit of MQDT is highly desirable, because the determination of the electron binding energies of Rydberg states by MQDT will ultimately be the limiting factor in our approach to determine the ionisation and dissociation energies of molecular hydrogen.

To reach this goal, we have implemented an improved method of determining the relative positions of the high-n Rydberg states of H_2 and their uncertainties from the millimetre-wave spectra, and restricted the analysis to the $np1_1$ ($S = 0$) Rydberg states. These states are much less sensitive to stray electric fields (see Fig. 3 of Ref. 22) and are not subject to predissociation nor to strong rotational channel interactions because they have negative electronic parity.[23] The widths of the corresponding lines were ~250 kHz, limited solely by the transit time of the molecules through the measurement region.

The relative positions of 33 $n = 54$–$64p1_1$ ($S = 0$) and 48 $n = 51$–$58d1_1$ ($G = 1$) Rydberg states were determined from the millimetre-wave spectra in a weighted linear least-squares fit of 248 observed transition frequencies using the method described in Ref. 24. The transition frequencies and their uncertainties were themselves obtained in weighted least-squares fits of sets of Gaussian line-shape functions to the observed spectra. The positions of the 33 $np1_1$ ($S = 0$) Rydberg states of H_2 with respect to the $51d1_1$ ($G^+ = \frac{1}{2}$, $G = 1$, $F = 0$) reference level determined in this way are listed in Table 3 with their statistical uncertainties given as one standard deviation. The root-mean-square (rms) deviation of these standard deviations is only 50 kHz which, we believe, represents the absolute accuracy of the measurement.
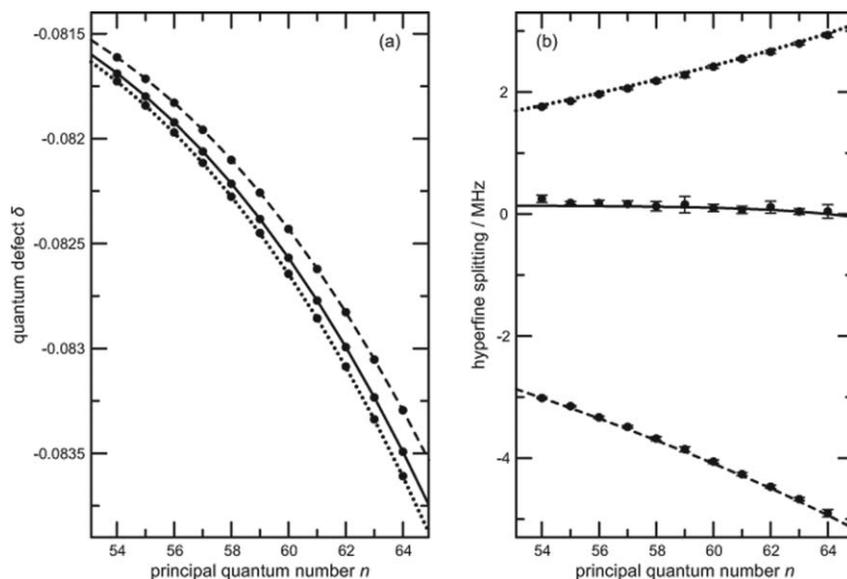
Fig. 3 Observed quantum defects [panel (a), determined using eqn (1)] and hyperfine splittings [panel (b)] of the $np1_1$ ($S = 0$) Rydberg series of H_2 as a function of n. The experimental standard deviations are indicated in panel (b) by vertical lines. The MQDT calculations of the $F = 0$, $F = 1$, and $F = 2$ hyperfine components are shown as solid, dashed, and dotted lines, respectively.

This journal is © The Royal Society of Chemistry 2011

The electron binding energies of these np Rydberg states were determined by MQDT using the procedure described in detail in Ref. 16 which considers all relevant rovibrational channel interactions (including p–f interactions) and the hyperfine interaction. The eigenquantum-defect functions were taken without changes from Ref. 16 except $\eta_{pp}^{S=0,\Lambda=1}(R)$ (R is the internuclear distance). The calculations also used the positions of the rovibrational levels and the hyperfine coupling parameters of H_2^+ reported in Ref. 10, 25 and Ref. 26–28, respectively. The basis set included p and f vibrational channels up to $v^+ = 6$ and 2, respectively. Test calculations with basis sets up to $v^+ = 15$ for the p channels confirmed that the calculated energies had converged to within 10 kHz and that the interactions of the np1_1 Rydberg states with the $2p\pi C^-$ and $3p\pi D^-$ dissociation continua can be neglected (see also discussion in Section V. C).

Rather than fitting the complete $\eta_{pp}^{S=0,\Lambda=1}(R)$ eigenquantum-defect function, only an R-independent correction $c_{pp}^{S=0,\Lambda=1}$ to the results reported in Ref. 16 and the electron binding energy E_{bind} of the $51d1_1$ ($G^+ = \frac{1}{2}$, $G = 1$, $F = 0$) reference level (relative to the centre of gravity of all hyperfine components of the X^+ ($v^+ = 0$, $N^+ = 1$) state of H_2^+) were adjusted in a least-square-fitting procedure. All relative energies listed in Table 3 could be reproduced with a rms deviation of 40 kHz using the improved values $c_{pp}^{S=0,\Lambda=1} = 1.08(11) \times 10^{-5}$ and $E_{bind}/hc = 42.3009108(14)$ cm^{-1}. Compared to the previous result $E_{bind}/hc = 42.300919(10)$ cm^{-1},[16] our new value represents an improvement in the uncertainty by a factor ~ 7, which suggests the possibility of improving the precision of future experimental determinations of the ionisation and dissociation energies of H_2, HD, and D_2 to better than 100 kHz, provided that the energy interval between the neutral ground state and high-n Rydberg states can be measured at that accuracy.

The experimental results are compared with the results of the MQDT calculations in Table 3 and Fig. 3. The dots in Fig. 3(a) show the quantum defect δ one obtains for each experimentally determined position using the Rydberg formula [eqn (1)]. In panel (b), the dots mark the three measured hyperfine components of each np1_1 ($S = 0$) Rydberg level. In both panels, the full, dashed, and dotted lines correspond to the results of the MQDT calculations, which quantitatively describe the experimental results. The following conclusions can be drawn from Fig. 3: First, panel (a) makes it obvious that the Rydberg formula cannot be used to extrapolate

Table 3 Observed and calculated np1_1 ($S = 0$) Rydberg states of *ortho*-H_2. E_{obs} is the observed energy relative to the $51d1_1$ state with $G^+ = \frac{1}{2}$, $G = 1$, and $F = 0$. δE_{obs} is the standard deviation of the observed energies and $\Delta_{obs-calc}$ is the difference between the observed and calculated energies

	$F = 0$			$F = 1$			$F = 2$		
n	E_{obs} (hc cm^{-1})	δE_{obs} (h kHz)	$\Delta_{obs-calc}$ (h kHz)	E_{obs} (hc cm^{-1})	δE_{obs} (h kHz)	$\Delta_{obs-calc}$ (h kHz)	E_{obs} (hc cm^{-1})	δE_{obs} (h kHz)	$\Delta_{obs-calc}$ (h kHz)
54	4.7919009	57	130	4.7917920	15	15	4.7919512	15	−9
55	6.1416218	23	43	6.1415107	12	24	6.1416775	11	−37
56	7.4197985	48	28	7.4196813	22	−5	7.4198580	19	−45
57	8.6313991	51	43	8.6312771	21	39	8.6314622	20	−31
58	9.7809676	78	48	9.7808405	34	67	9.7810361	27	20
59	10.8726673	136	21	10.8725336	41	23	10.8727382	41	−55
60	11.9103197	58	−4	11.9101810	28	30	11.9103969	27	−21
61	12.8974358	59	−4	12.8972913	28	41	12.8975184	23	5
62	13.8372458	98	38	13.8370929	25	16	13.8373307	24	−34
63	14.7327216	47	4	14.7325644	27	40	14.7328135	23	−21
64	15.5866119	111	−1	15.5864470	61	−7	15.5867084	40	−68
rms		76	48	rms	31	33	rms		26	36

to the series limit because the quantum defects depend on the principal quantum number. Second, the figure shows that the hyperfine splittings themselves are strongly n-dependent, which indicates that the hyperfine structure of the H_2^+ ion significantly differs from that of the $np1_1$ ($S = 0$) Rydberg states. Finally, the analysis of the calculations enables one to attribute the reduction of the observed quantum defects which increased n values to the increasing singlet–triplet mixing induced by the hyperfine interaction. The reason why the MQDT calculations properly account for the observations is that the treatment includes singlet ($S = 0$) and triplet ($S = 1$) channels and the hyperfine interactions in the H_2^+ ion.

IV. Next generation of measurements

In the previous section we demonstrated that the high-$n \rightarrow X^+$ interval can be determined with an accuracy of better than 100 kHz. In this section, we discuss the possibility of measuring the energies of high-n Rydberg states of molecular hydrogen with respect to the ground state at the same accuracy. The uncertainty ΔE of the electron binding energy of a given Rydberg state determined with optimised MQDT parameters can be estimated from the uncertainty of the eigenquantum-defect functions. For the $np1_1$ ($S = 0$) series discussed in the previous section, ΔE may be estimated from the uncertainty $\Delta c_{\mathrm{pp}}^{S=0,\Lambda=1} = 1.1 \times 10^{-6}$ using

$$\frac{\Delta E}{hc} = \frac{2R_M \Delta c_{\mathrm{pp}}^{S=0,\Lambda=1}}{n^3}. \tag{3}$$

At $n = 54$, this uncertainty corresponds to 45 kHz. At n values of 20 and 10, it increases to 0.9 MHz and 7.2 MHz, respectively. Although eqn (3) suggests that measurements at higher n values than 64 should result in smaller uncertainties, such measurements are complicated by the fact that the systematic uncertainties rapidly become limited by Stark shifts induced by stray electric fields and that the transition moments from the ground state or from low-lying electronic states scale as $n^{-3/2}$. The range of principal quantum numbers 50–60 thus represents an optimal compromise. Such Rydberg states lie more than 124 000 cm^{-1} above the $X\ ^1\Sigma_g^+$ ground state.

For simplicity, we focus on H_2, but similar considerations also apply to HD and D_2. We discuss the case of *para*-H_2, although the latest measurement has been carried out with *ortho*-H_2. The hyperfine structure of the X and EF states, which is absent in *para*-H_2, could lead to complicated line shapes at higher resolution.

The conceptually simplest approach to determine absolute energies of the high-n Rydberg states involves direct transitions from the ground state using single-photon excitation with extreme-ultraviolet (XUV) laser radiation, or nonresonant multiphoton excitation using UV radiation [Fig. 4(d)]. Unfortunately, neither of these approaches appears very promising at present. Nonresonant multiphoton excitation to high-n Rydberg states is notoriously difficult and requires high intensities, which would inevitably lead to systematic uncertainties because of ac Stark shifts. Moreover, ionisation processes would be very difficult to avoid and the inhomogeneous electric fields caused by the ions in the experimental volume would lead to undesirable inhomogeneous line broadening and line shifts. Single-photon XUV metrology at an absolute accuracy of better than 100 kHz would necessitate the use of XUV frequency combs.[29] However, the high density of Rydberg states at high n values precludes such measurements. Although the application of dual-frequency-comb spectroscopy, which has been shown to be able to resolve dense molecular spectra,[30] may enable one to overcome this problem, it appears beyond reach at present. Moreover, several comb lines would inevitably have frequencies above the ionisation threshold which, in turn, would lead to undesirable ions in the excitation volume and to considerable systematic uncertainties.

In the following, we thus restrict the discussion to experimental schemes which divide the $X \rightarrow$ high-n interval into several intervals. Such excitation schemes
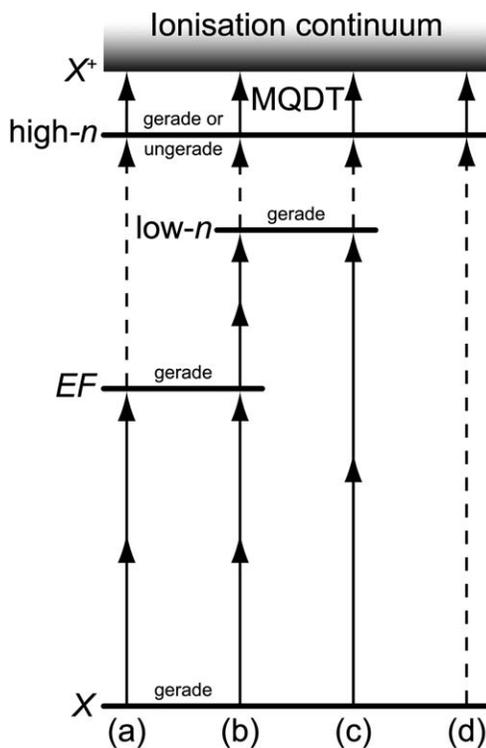
Fig. 4 Segmentation of the ionisation energy of molecular hydrogen into several energy intervals leading to four proposed measurement schemes: (a) $X \to EF \to$ high-$n \to X^+$, (b) $X \to EF \to$ low-$n \to$ high-$n \to X^+$, (c) $X \to$ low-$n \to$ high-$n \to X^+$, and (d) $X \to$ high-$n \to X^+$. Solid double arrows are used for intervals which can only be measured with a two-photon transition for symmetry reasons. Intervals indicated by dashed arrows can either be measured with a one- or two-photon transition (see Section IV for a detailed discussion of these schemes).

require intermediate levels with a sufficiently narrow natural linewidth unless the intermediate level is coherently coupled to the long-lived high-n Rydberg states using a slightly detuned laser pulse. We exclude such schemes from our considerations because the weak intensity of XUV sources makes nonresonant two-photon excitation very difficult. If one assumes that a natural linewidth $\Delta \nu < 1$ MHz (full width at half maximum) of an intermediate level is necessary to measure the corresponding spectral position with an absolute accuracy of less than 100 kHz, only states with a minimal lifetime of

$$\tau = \frac{1}{2\pi\Delta\nu} = 160 \text{ ns} \qquad (4)$$

need to be considered. A review of the lifetimes of low-lying electronically excited states of molecular hydrogen has been published in Ref. 31 and the singlet states with the longest lifetimes are listed in Table 4. Only the $2s\sigma EF$ ($v = 0$) state meets the requirement imposed by eqn (4). In addition, a lifetime of slightly more than 160 ns has been measured for the $4s\sigma O$ state.[32] The radiative lifetimes of higher excited states directly accessible from the ground state have to our knowledge not been measured but can be estimated by comparing with the corresponding states of atomic helium.[33] The comparison suggests that ns states with $n \geq 6$, np states with $n \geq 14$, and nd states with $n \geq 7$ fulfill eqn (4). However, the lifetimes of molecular states differ because of the ν^3 dependence of the Einstein A coefficient, predissociation, s/d mixing or small Franck–Condon factors. Given that all p states

Table 4 A selection of excited gerade states of molecular hydrogen, which could be used as intermediate states in future measurements of the adiabatic ionisation energy of H_2, HD, and D_2. The energy is given for H_2 relative to the X ($v = 0$, $N = 0$) rovibronic ground state. $\Delta\nu$ is the natural linewidth [see eqn (4)]. $\lambda_X^{(2)}$ and $\lambda_{EF}^{(2)}$ are the wavelengths needed for a two-photon excitation from the X (0,0) and EF (0,0) states, respectively and $\lambda_{n=60}^{(1)}$ is the wavelength needed for a one-photon excitation to a $n = 60$ Rydberg state. Columns denoted by FCF contain the corresponding Franck–Condon factors.[99]

Name	Label[a]	Energy (hc cm^{-1})	Ref.	$\Delta\nu$ (MHz)	Ref.	$\lambda_X^{(2)}$ (nm)	FCF	$\lambda_{EF}^{(2)}$ (nm)	FCF	$\lambda_{n=60}^{(1)}$ (nm)	FCF
EF	2sσ (0,0)	99 164.78691(11)	15	0.8	36	202	0.158			396	0.965
EF	2sσ (1,0)	99 363.8876(4)	45	0.1	100	201	0.000			400	0.000
EF	2sσ (2,0)	100 558.8516(10)	45	0.2	100	199	0.000			420	0.000
EF	2sσ (3,0)	101 494.74402(15)	45	1.2	36	197	0.216			437	0.035
H	3sσ (0,0)	112 957.5598(10)	45	1.4	100	177	0.109	1450	0.984	875	0.996
H	3sσ (1,0)	115 251.5024(50)	45	2.0	100	174	0.181	1243	0.015	1095	0.004
O	4s0$_0$	117 886.34(6)	32	0.9	32	170	0.099	1068	0.976	1538	0.999
	5s0$_0$	120 195	101			166	0.091	951	0.965	2385	1.000
	6s0$_0$	121 479	101			165	0.091	896	0.965	3439	1.000
	7d0$_2$	122 163	101			164	0.091	870	0.965	4496	1.000
	7s0$_0$	122 240	101			164	0.091	867	0.965	4657	1.000
	8d0$_2$	122 690.5	101			163	0.091	850	0.965	5894	1.000
	8s0$_0$	122 744.2	101			163	0.091	848	0.965	6087	1.000
	9d0$_2$	123 054.1	101			163	0.091	837	0.965	7502	1.000
	9s0$_0$	123 090.9	101			162	0.091	836	0.965	7715	1.000
	10d0$_2$	123 313	101			162	0.091	828	0.965	9310	1.000
	10s0$_0$	123 341.4	101			162	0.091	827	0.965	9563	1.000

[a] Notation: $n\ell\lambda$ (v,N) for the EF and H states and $n\ell N_N^+$ otherwise. All quantum numbers have their usual meanings (see, *e.g.*, Table 1 in Ref. 16).

with a natural linewidth of less than 1 MHz are expected to lie less than $\sim R_M/14^2 = 560$ cm^{-1} below the ionisation limit and the excitation of states with $\ell \geq 3$ from the X, EF, H or O states is dipole forbidden, only s and d states are considered as possible intermediate states.

These considerations reduce the number of possible excitation schemes to three (see Fig. 4): (a) $X \rightarrow EF \rightarrow$ high-n, (b) $X \rightarrow EF \rightarrow$ low-$n \rightarrow$ high-n, and (c) $X \rightarrow$ low-$n \rightarrow$ high-n. Table 4 contains a list of possible EF and low-n ($n \leq 10$) inter-mediate states with selected spectroscopic properties and forms the basis of the following discussion of measurements of the different energy intervals in the three excitation schemes.

A. The $X \rightarrow EF$ interval

The data presented on the EF state in Table 4 indicates that the X ($v = 0$) $\rightarrow EF$ ($v = 0$) transition is the most favourable as far as lifetime and two-photon excitation frequency are concerned. The X ($v = 0$) $\rightarrow EF$ ($v = 1,2$) transitions can be ruled out because of the zero Franck–Condon factors resulting from the fact that the vibrational wavefunction is primarily localised in the outer (F) well. The X ($v = 0$) $\rightarrow EF$ ($v = 3$) transition has a good Franck–Condon factor (0.2) but a reduced lifetime and a frequency at the limit of what can be reached by frequency upconversion in β-barium borate (BBO) crystals. Moreover, the Franck–Condon factors for transitions to Rydberg states are reduced compared to the EF ($v = 0$) state. We thus conclude that the EF ($v = 0$) state is the most attractive candidate for the measurement of the $X \rightarrow EF$ interval.

Because the EF state is of gerade symmetry, nonresonant two-photon excitation is the only option. A counterpropagating arrangement enables Doppler-free

measurements as already exploited in the most recent measurements of this interval.[15,34] These measurements have relied on amplified and frequency-upconverted nanosecond laser pulses, and were limited so far to an accuracy of several MHz by frequency-chirping effects, which will be difficult to further reduce.[15] The use of long pulses (100 ns or more are possible[35]) might be considered as an alternative though it is uncertain that a 100 kHz accuracy can be reached in this way. A careful control of ac Stark shifts and residual Doppler shifts is in any case mandatory for any experiment. The accuracy of a measurement of this interval will ultimately be limited to ∼80 kHz by the natural linewidth of the $EF(v = 0)$ state which is 800 kHz.[36]

The most promising alternatives to an excitation using nanosecond laser pulses are cw UV laser radiation and direct two-photon frequency-comb spectroscopy. The former appears demanding in terms of cw power. The generation of intense 202 nm laser light could be achieved by cavity-enhanced cw frequency tripling in BBO crystals. This technique has already been applied to produce up to 175 mW and 10 mW cw radiation near 272 nm (Ref. 37) and 227 nm (Ref. 38), respectively. As the phase-matching cutoff for third-harmonic generation (THG) in BBO crystals is at 196 nm it should in principle be possible to use the same technique at 202 nm although a lower efficiency of the THG might pose additional problems.[39] Note that it is not possible to obtain 202 nm radiation by frequency doubling in a BBO crystal because the phase-matching cutoff for this process is at 204.8 nm.[40]

Frequency-comb lasers are increasingly used for calibration and stabilisation of UV, visible, and infrared laser radiation with an accuracy and stability of better than 100 kHz. The output of a frequency-comb laser can also be used to excite and measure states of atoms and molecules, using a technique referred to as direct frequency-comb spectroscopy (DFCS). A few years ago, DFCS was demonstrated in the vacuum ultraviolet (VUV) with sub-MHz accuracy.[41,42] This technique also opens new perspectives for precision spectroscopy in molecules, although additional difficulties arise from the higher density of states and the lower transition moments. The $X \rightarrow EF$ transition may be a good candidate for the application of Doppler-free DFCS to molecular hydrogen because the EF state is relatively isolated. Pulses with a wavelength around 202 nm could be produced by fourth-harmonic generation of the output of a Ti:Sa frequency-comb laser in three successive BBO crystals.[15] The bandwidth of the comb would have to be carefully chosen so that only the vibrational ground state of the EF state is excited, but no higher vibrational states, because their excitation would perturb the measurement.

B.   The $X \rightarrow$ low-n interval

Given that the long-lived low-n states in Table 4 are of gerade symmetry, only two-photon excitation needs to be considered for the measurement of the $X \rightarrow$ low-n interval. Transitions to the low-n states ($n \geq 3$) would need radiation with wavelengths shorter than 177 nm, which cannot be generated in nonlinear crystals. The VUV radiation would need to be produced by four-wave mixing in carefully phase-matched nonlinear gas cells. The 1s–2s transition in He has been measured by two-photon Doppler-free spectroscopy using radiation near 120 nm,[43] which indicates that such measurements should also be possible in molecular hydrogen. However, the accuracy reached in the He 1s–2s measurement was limited to 48 MHz by the extrapolation of the ac Stark shift to zero intensity. It thus seems unlikely that a precision of 100 kHz could be reached in a measurement of the $X \rightarrow$ low-n interval in this way, and we believe that this interval is best determined in two steps as a sum of the $X \rightarrow EF(v = 0)$ and $EF(v = 0) \rightarrow$ low-n intervals.

C.   The $EF \rightarrow$ low-n interval

The EF and X states have the same electronic symmetry so that a measurement of the $EF \rightarrow$ low-n interval also imposes the use of a Doppler-free two-photon

excitation scheme. The wavelengths of these transitions lie in the range between 1500 nm and 800 nm, where powerful cw laser sources are available, *e.g.* Ti:Sa lasers, diode lasers and optical parametric oscillators. Moreover, the two-photon transitions from the *EF* state to low-*n* Rydberg states are expected to be much stronger than those to the high-*n* Rydberg states. A high-accuracy measurement of this interval thus seems feasible with current technologies. In order to determine the ionisation and dissociation energies of molecular hydrogen, an independent measurement of the low-*n* → high-*n* interval is required.

D. The *EF* → high-*n* interval

The accuracy of the measurement of the *EF* → high-*n* interval by single-photon excitation presented in Section II is limited by the Doppler width, which is substantial at 400 nm, even when a skimmed supersonic beam of molecular hydrogen is used. It is unlikely that improvements of the collimation, *e.g.* by the use of a double skimmer, would enable the desired reduction of linewidth to a value less than 1 MHz. The use of cold samples of molecular hydrogen may, in future, lead to a sufficient reduction of the Doppler width. At present, stationary samples of H_2 Rydberg molecules with a temperature of 100 mK can be produced,[44] corresponding to a Doppler width of 120 MHz at 400 nm. Further cooling to 7 μK or convenient phase-space manipulation would be required to reduce the Doppler width below 1 MHz, which is currently out of reach. The selection of a narrow velocity component in the two-photon $X \rightarrow EF$ transition represents an alternative to reduce the Doppler width of the *EF* → high-*n* transition.

Here again, Doppler-free two-photon spectroscopy represents the most attractive route to a precision measurement of high-*n* gerade Rydberg states. For this interval, it does not matter whether transitions to gerade or ungerade high-*n* Rydberg states are measured because both are long-lived and the relative positions can be measured with high accuracy using millimetre-wave spectroscopy. Ideal would be a measurement with cw laser radiation near 800 nm, but such a measurement would require intensities at the limit of what is currently possible. As there are no suitable ungerade levels midway between the *EF* and the high-*n* Rydberg states (the closest being the $3p\sigma B'$ ($v = 1$, $N = 1$) state which is more than 500 cm^{-1} off[45]), enhancements of the two-photon transition moment by near-resonant intermediate states are expected to be minimal. The pulse-amplified output of our Ti:Sa laser system, with pulse lengths adjustable to beyond 100 ns,[35] may represent an alternative. Care would have to be taken to monitor and compensate the frequency chirp and shift occurring in the amplification process, as described, *e.g.*, in Ref. 46. One would also have to carefully quantify the pressure shifts of the high-*n* Rydberg states and the ac Stark shifts of these states induced by blackbody radiation.

Doppler-free measurements of transitions to high-*n* states have to our knowledge only been measured from ground-state atoms in a room-temperature gas cell, see, *e.g.*, Ref. 47, 48. Given that the *EF* state can be excited using cw radiation the measurements described in this section could also be performed in a cell of molecular hydrogen. Such an arrangement would provide a larger sample than using a supersonic beam but the pressure, Stark, and Zeeman shifts would be more difficult to determine at the required precision.

E. The low-*n* → high-*n* interval

The low frequency of the low-*n* → high-*n* transition reduces the uncertainty associated with the Doppler broadening, and this interval could be measured with a one-photon transition at high accuracy using a well-collimated molecular beam. The selection of a narrow range of velocity components could be achieved by carrying out the excitation from the *X* ground state to the gerade low-*n* state *via* the ungerade 2pσB state with narrow-band lasers and would lead to a further reduction of the Doppler width.

V. The limits of purely *ab initio* MQDT

At present the precision and accuracy of the ionisation and dissociation energies of molecular hydrogen is not limited by the uncertainty in the determination of the electron binding energy of the high-n Rydberg states by MQDT-assisted millimetre-wave spectroscopy, but by that of the $X \rightarrow$ high-n interval. The statistical uncertainty of 45 kHz given for the high-$n \rightarrow X^+$ interval determined in Section III relies on the assumption that systematic errors originating from the approximations in the MQDT treatment are eliminated in the least-squares fitting procedure. MQDT-assisted millimetre-wave spectroscopy, although it relies on *ab initio* parameters, leads to effective parameters obtained in a least-squares fit to experimentally determined positions. We complete this article by discussing the current limits of purely *ab initio* MQDT and how these limits might be overcome in future. One additional virtue of an improved purely *ab initio* theory for the determination of E_i and D_0 is that it will facilitate the accurate determination of the electron binding energies of Rydberg states of lower principal quantum numbers than those with n in the range 50–65 upon which our current (Sections II and III) and the proposed improved (Section IV) schemes rely. The experimental measurement of the $EF \rightarrow$ high-n and low-$n \rightarrow$ high-n intervals could then be carried out more easily because of the n^{-3} scaling of the intensities of transitions from low-lying electronic states to high-n Rydberg states.

Improvements of purely *ab initio* MQDT can be achieved in three main directions by (1) improving clamped-nuclei eigenquantum-defect functions, (2) reducing the possible uncertainties resulting from the frame-transformation approximation, and (3) including more complete vibrational basis sets for the cations which also include the dissociation continuum.

A. Clamped-nuclei eigenquantum defects

The obvious desideratum for improvements on the theoretical side would be to achieve the same theoretical accuracy *ab initio* as envisioned here for future experiments. Eqn (3) implies that, for calculations at $n \approx 50$, the eigenquantum defects must be predicted with an accuracy of better than 10^{-6}. For comparison, at the $n = 2$ level, where the lowest Rydberg states are situated, an eigenquantum defect of this accuracy would allow one to predict energy levels correctly to within 0.03 cm^{-1}. The presently best *ab initio* predictions for the lowest Rydberg states of H_2 do not quite reach this level of accuracy, but are not far from it.

For instance, the best existing potential energy curve for a member of the $np\pi$ ($S = 0$) Rydberg series was published by Wolniewicz and Staszewska for the $2p\pi C$ state.[49] Based on this clamped-nuclei curve, the level $2p\pi C^-$ ($v = 0$, $N = 1$) has been predicted to lie 0.45 cm^{-1} above the experimental value in a fully *ab initio* coupled-equations approach,[50] whereas MQDT, with an eigenquantum-defect function extracted from the same clamped-nuclei curve and using the frame-transformation method, predicts the same level to lie 0.14 cm^{-1} below the experimental value.[51]

Unfortunately, accurate quantum-chemical calculations of the type of Ref. 49 are not possible presently for states beyond $n \approx 5$, because of inherent convergence problems arising in the computations. No significant improvement of this situation is in sight as far as we are aware. Calculations based on scattering theory, using the Kohn or Schwinger variational principles, are designed specifically to deal with states in or near the electronic continuum, and may constitute an alternative. R-matrix as well as Feshbach/B-spline-formalism computations on H_2 have indeed been published,[52–54] but they were carried out to explore the broad electron-ion resonances occurring in the continuum, rather than to achieve high accuracy. In Ref. 53, clamped-nuclei eigenquantum-defects were obtained for singlet ungerade symmetry that are accurate to within better than $\sim 3 \times 10^{-2}$, which is four orders of magnitude larger than the present requirement. However, the results presented in Ref. 53 had

the character of proof-of-principle computations carried out with rather small basis sets, and there appears to be room for considerable improvement if more carefully designed basis sets are employed. Unlike more conventional quantum-chemical calculations, these results retain their accuracy over a wide range of energies, and are actually more adapted to the calculation of high-n than low-n Rydberg states.

Even if highly precise calculations of clamped-nuclei eigenquantum defects were not possible, they may help to improve the MQDT model used in the present work because they should allow us to include more electron-ion channels explicitly in the calculations. The calculations of levels of ungerade symmetry reported in Section III include explicitly only the $(1\sigma_g)\varepsilon p\lambda$ and $(1\sigma_g)\varepsilon f\lambda$ channels, but neglect the lowest core-excited $(1\sigma_u)\varepsilon s\lambda$ and $(1\sigma_u)\varepsilon d\lambda$ as well as higher configurations in the asymptotic region. The latter are of course included in an effective manner in the present treatment (and *via* the configuration-interaction expansion inside the reaction zone of a clamped-nuclei R-matrix calculation[53]), but their explicit inclusion should lead to more accurate level positions, even when only the $(1\sigma_g)\varepsilon p\lambda$ and $(1\sigma_g)\varepsilon f\lambda$ eigenquantum defects are adjusted to fit the experimental measurements.

B.   Frame transformation

As already mentioned in Section III, the frame transformation used in the current version of MQDT to take nonadiabatic effects into account constitutes an approximation, the quality of which is difficult to assess. It is based on the assumption that the Coulomb radial wave functions of the Rydberg electron are strictly energy-independent in the core region. The frame transformation is therefore taken as an energy-independent matrix, whereas in reality it should depend – albeit only weakly – on the total energy of the molecule, just like any reaction matrix or phase shift in scattering theory. Improvements to the original formalism of Fano[55] have been made, including a number of small correction terms,[56] and in particular an energy-modified adiabatic nuclei approximation.[9,57] These corrections introduce an energy dependence in an effective way and they are essential, for Rydberg states with $n < 5$, to achieve agreement between experiment and *ab initio* theory in the order of 1 (or a few) cm^{-1}.[51,56]

Gao and Greene[58] have proposed an R-matrix-like matching procedure on the core boundary of short-range (Born–Oppenheimer) and asymptotic (nonadiabatic) Rydberg-wavefunction expansions which, in principle at least, takes full account of energy dependences. Their theory constitutes a promising extension of molecular MQDT and contains the standard frame transformation as a limiting case. Their formalism has not been implemented in a systematic way yet, mainly because it implies a substantially increased numerical effort, so that some of the simplicity of MQDT is lost. A creative compromise between the two limiting theories would certainly lead to significant progress.

C.   Vibrational basis sets and molecular dissociation

The last of the present limitations of MQDT which we mention here concerns the ion-core vibrational basis sets. The vibrational basis used in the present work is not complete. The basis was chosen so that the main low-n and high-v perturbers are correctly described. These interact in a specific way with the high-n $v = 0$ Rydberg series of interest, and must therefore be well described. Remaining effects of the incomplete basis sets are absorbed by the least-squares fitting procedure, although we are not in a position at present to prove it.

If the vibrational basis is extended to high vibrational quantum numbers, it will eventually extend into the dissociation continuum of the ion core. Given the fact that the ion core vibrational wavefunction is calculated over a finite range of internuclear distances, a large number of quasi-discrete vibrational wavefunctions will be produced (*cf. e.g.* Fig. 13 of Ref. 9), which represent the discretised dissociation

continuum of the ion core. This ion-core quasi-continuum is converted *via* the MQDT procedures into one (or several) molecular dissociation quasi-continua. Their structure poses a problem because it perturbs the level structure of interest in an unpredictable fashion. However, these perturbations may in turn be used to calculate predissociation widths and shifts of the Rydberg series of interest.[23,59] Combining these ideas with the present MQDT approach should lead to an improved accuracy of the theoretical calculations. Their implementation represents a technical rather than a conceptual problem.

In future we expect that the development of purely *ab initio* MQDT along the lines described above will be beneficial to the determination of E_i and D_0 at ever increasing accuracy. Because of the necessity of each improvement in the theory to be rigorously tested by experiments, improved experimental methods for high-resolution spectroscopy of high-n Rydberg states are also desirable.

VI.   Conclusions

Recent experimental progress in the determination of the adiabatic ionisation energy (E_i) and the dissociation energy (D_0) of molecular hydrogen has enabled a stringent test of *ab initio* calculations and the validation of the various calculated contributions (electron correlation, and adiabatic, nonadiabatic, relativistic, and QED corrections) of these energies. At present, experimental and theoretical values of the adiabatic ionisation and dissociation energies agree within the reported uncertainties of the calculations as estimated from the magnitude of the highest-order correction terms evaluated to date (0.001 cm^{-1} or 30 MHz, *i.e.*, 8×10^{-9} relative accuracy for E_i and 3×10^{-8} relative accuracy for D_0).

The determination of the electron binding energies of high-n Rydberg states (principal quantum number $n \approx 60$) is an essential step of the experimental procedure to determine E_i and D_0 and will eventually limit their precision and accuracy. We have shown in this article that the electron binding energies of gerade and ungerade high-n Rydberg states of H_2 can be determined with an accuracy slightly better than 100 kHz using a combination of millimetre-wave spectroscopy and multichannel quantum-defect theory. This result opens up the prospect of carrying out a new determination of the ionisation and dissociation energies of molecular hydrogen by remeasuring the $X \rightarrow$ high-n interval with improved accuracy. By evaluating possible schemes to determine this interval, the segmentation into three excitation steps [$X \rightarrow EF$, $EF \rightarrow$ low-n, and low-$n \rightarrow$ high-n, see Fig. 4(b)] appears particularly promising. The ultimate accuracy limit in the range 50–100 kHz of this scheme is almost two orders of magnitude better than the accuracy of the current best result (see Fig. 1) and approaches the fundamental limit for theoretical values of about 10 kHz imposed by the current uncertainty of the proton-to-electron mass ratio.

Acknowledgements

References

1 W. Kołos and L. Wolniewicz, *J. Chem. Phys.*, 1968, **49**, 404–410.
2 P. Maksyutenko, Th. R. Rizzo and O. V. Boyarkin, *J. Chem. Phys.*, 2006, **125**, 181101.

3 Y. P. Zhang, C. H. Cheng, J. T. Kim, J. Stanojevic and E. E. Eyler, *Phys. Rev. Lett.*, 2004, **92**, 203003.

4 R. G. Neuhauser, K. Siglow and H. J. Neusser, *J. Chem. Phys.*, 1997, **106**, 896–907.

5 R. Seiler, U. Hollenstein, G. M. Greetham and F. Merkt, *Chem. Phys. Lett.*, 2001, **346**, 201–208.

6 R. Seiler, U. Hollenstein, T. P. Softley and F. Merkt, *J. Chem. Phys.*, 2003, **118**, 10024–10033.

7 A. Osterwalder, S. Willitsch and F. Merkt, *J. Mol. Struct.*, 2001, **599**, 163–176.

8 *Molecular Applications of Quantum Defect Theory*, ed. Ch. Jungen, Institute of Physics Publishing, Bristol and Philadelphia, 1996.

9 Ch. Jungen, Elements of Quantum Defect Theory, in *Handbook of High-resolution Spectroscopy*, ed. M. Quack and F. Merkt, Wiley & Sons, 2011.

10 V. I. Korobov, *Phys. Rev. A: At., Mol., Opt. Phys.*, 2008, **77**, 022509, and references therein.

11 P. J. Mohr, B. N. Taylor and D. B. Newell, *Rev. Mod. Phys.*, 2008, **80**, 633–730, see: http://physics.nist.gov/hdel for numerical values.

12 J. Liu, E. J. Salumbides, U. Hollenstein, J. C. J. Koelemeij, K. S. E. Eikema, W. Ubachs and F. Merkt, *J. Chem. Phys.*, 2009, **130**, 174306.

13 D. Sprecher, J. Liu, Ch. Jungen, W. Ubachs and F. Merkt, *J. Chem. Phys.*, 2010, **133**, 111102.

14 J. Liu, D. Sprecher, Ch. Jungen, W. Ubachs and F. Merkt, *J. Chem. Phys.*, 2010, **132**, 154301.

15 S. Hannemann, E. J. Salumbides, S. Witte, R. T. Zinkstok, E.-J. van Duijn, K. S. E. Eikema and W. Ubachs, *Phys. Rev. A: At., Mol., Opt. Phys.*, 2006, **74**, 062514.

16 A. Osterwalder, A. Wüest, F. Merkt and Ch. Jungen, *J. Chem. Phys.*, 2004, **121**, 11810–11838.

17 H. A. Cruse, Ch. Jungen and F. Merkt, *Phys. Rev. A: At., Mol., Opt. Phys.*, 2008, **77**, 042502.

18 K. Piszczatowski, G. Łach, M. Przybytek, J. Komasa, K. Pachucki and B. Jeziorski, *J. Chem. Theory Comput.*, 2009, **5**, 3039–3048.

19 K. Pachucki and J. Komasa, *Phys. Chem. Chem. Phys.*, 2010, **12**, 9188–9196.

20 K. Pachucki, *Phys. Rev. A: At., Mol., Opt. Phys.*, 2006, **74**, 022512.

21 G. Herzberg, *J. Mol. Spectrosc.*, 1970, **33**, 147–168.

22 A. Osterwalder, R. Seiler and F. Merkt, *J. Chem. Phys.*, 2000, **113**, 7939–7944.

23 M. Glass-Maujean, Ch. Jungen, G. Reichardt, A. Balzer, H. Schmoranzer, A. Ehresmann, I. Haar and P. Reiss, *Phys. Rev. A: At., Mol., Opt. Phys.*, 2010, **82**, 062511.

24 M. Schäfer and F. Merkt, *Phys. Rev. A: At., Mol., Opt. Phys.*, 2006, **74**, 062506.

25 R. E. Moss, *Mol. Phys.*, 1993, **80**, 1541–1554.

26 V. I. Korobov, L. Hilico and J.-Ph. Karr, *Phys. Rev. A: At., Mol., Opt. Phys.*, 2006, **74**, 040502(R).

27 V. I. Korobov, L. Hilico and J.-Ph. Karr, *Phys. Rev. A: At., Mol., Opt. Phys.*, 2009, **79**, 012501.

28 Z.-X. Zhong, Z.-C. Yan and T.-Y. Shi, *Phys. Rev. A: At., Mol., Opt. Phys.*, 2009, **79**, 064502.

29 D. Z. Kandula, Ch. Gohle, T. J. Pinkert, W. Ubachs and K. S. E. Eikema, *Phys. Rev. Lett.*, 2010, **105**, 063001.

30 B. Bernhardt, A. Ozawa, P. Jacquet, M. Jacquey, Y. Kobayashi, Th. Udem, R. Holzwarth, G. Guelachvili, T. W. Hänsch and N. Picqué, *Nat. Photonics*, 2010, **4**, 55–57.

31 S. A. Astashkevich and B. P. Lavrov, *Opt. Spectrosc.*, 2002, **92**, 818–850.

32 H. Aita, Y. Ogi and K. Tsukiyama, *J. Mol. Spectrosc.*, 2005, **232**, 315–322.

33 C. E. Theodosiou, *At. Data Nucl. Data Tables*, 1987, **36**, 97–127.

34 A. Yiannopoulou, N. Melikechi, S. Gangopadhyay, J. C. Meiners, C. H. Cheng and E. E. Eyler, *Phys. Rev. A: At., Mol., Opt. Phys.*, 2006, **73**, 022506.

35 R. Seiler, Th. Paul, M. Andrist and F. Merkt, *Rev. Sci. Instrum.*, 2005, **76**, 103103.

36 D. W. Chandler and L. R. Thorne, *J. Chem. Phys.*, 1986, **85**, 1733–1737.

37 J. Mes, E. J. van Duijn, R. Zinkstok, S. Witte and W. Hogervorst, *Appl. Phys. Lett.*, 2003, **82**, 4423.

38 J. Shao, L. Lathdavong, P. Thavixay and O. Axner, *J. Opt. Soc. Am. B*, 2007, **24**, 2294–2306.

39 D. Eimerl, L. Davis, S. Velsko, E. K. Graham and A. Zalkin, *J. Appl. Phys.*, 1987, **62**, 1968–1983.

40 S. Bourzeix, B. de Beauvoir, F. Nez, F. de Tomasi, L. Julien and F. Biraben, *Opt. Commun.*, 1997, **133**, 239–244.

41 S. Witte, R. Th. Zinkstok, W. Ubachs, W. Hogervorst and K. S. E. Eikema, *Science*, 2005, **307**, 400–403.

This journal is © The Royal Society of Chemistry 2011

42 R. Th. Zinkstok, S. Witte, W. Ubachs, W. Hogervorst and K. S. E. Eikema, *Phys. Rev. A: At., Mol., Opt. Phys.*, 2006, **73**, 061801(R).
43 S. D. Bergeson, A. Balakrishnan, K. G. H. Baldwin, T. B. Lucatorto, J. P. Marangos, T. J. McIlrath, T. R. O'Brian, S. L. Rolston, C. J. Sansonetti, J. Wen, N. Westbrook, C. H. Cheng and E. E. Eyler, *Phys. Rev. Lett.*, 1998, **80**, 3475–3478.
44 S. D. Hogan, Ch. Seiler and F. Merkt, *Phys. Rev. Lett.*, 2009, **103**, 123001.
45 D. Bailly, E. J. Salumbides, M. Vervloet and W. Ubachs, *Mol. Phys.*, 2010, **108**, 827–846.
46 K. S. E. Eikema, W. Ubachs, W. Vassen and W. Hogervorst, *Phys. Rev. A: At., Mol., Opt. Phys.*, 1997, **55**, 1866–1884.
47 S. A. Lee, J. Helmcke, J. L. Hall and B. P. Stoicheff, *Opt. Lett.*, 1978, **3**, 141–143.
48 P. Thoumany, T. Hänsch, G. Stania, L. Urbonas and Th. Becker, *Opt. Lett.*, 2009, **34**, 1621–1623.
49 L. Wolniewicz and G. Staszewska, *J. Mol. Spectrosc.*, 2003, **220**, 45–51.
50 L. Wolniewicz, T. Orlikowski and G. Staszewska, *J. Mol. Spectrosc.*, 2006, **238**, 118–126.
51 M. Glass-Maujean, Ch. Jungen, M. Roudjane and W.-L. Tchang-Brillet, in preparation.
52 J. Tennyson, *At. Data Nucl. Data Tables*, 1996, **64**, 253–277.
53 M. Telmini and Ch. Jungen, *Phys. Rev. A: At., Mol., Opt. Phys.*, 2003, **68**, 062704.
54 I. Sánchez and F. Martín, *J. Chem. Phys.*, 1997, **106**, 7720–7730.
55 U. Fano, *Phys. Rev. A: At., Mol., Opt. Phys.*, 1970, **2**, 353–365.
56 S. C. Ross and Ch. Jungen, *Phys. Rev. A: At., Mol., Opt. Phys.*, 1994, **49**, 4364–4377.
57 R. K. Nesbet, *Phys. Rev. A: At., Mol., Opt. Phys.*, 1979, **19**, 551–556.
58 H. Gao and C. H. Greene, *Phys. Rev. A: At., Mol., Opt. Phys.*, 1990, **42**, 6946–6949.
59 Ch. Jungen and S. C. Ross, *Phys. Rev. A: At., Mol., Opt. Phys.*, 1997, **55**, R2503–R2506.
60 L. Wolniewicz, *J. Chem. Phys.*, 1993, **99**, 1851–1868.
61 T. Orlikowski, G. Staszewska and L. Wolniewicz, *Mol. Phys.*, 1999, **96**, 1445–1448.
62 L. Wolniewicz and K. Dressler, *J. Chem. Phys.*, 1994, **100**, 444–451.
63 L. Wolniewicz, *J. Chem. Phys.*, 1998, **108**, 1499.
64 D. M. Bishop and R. W. Wetmore, *Mol. Phys.*, 1973, **26**, 145–157.
65 E. E. Witmer, *Phys. Rev.*, 1926, **28**, 1223–1241.
66 W. Heitler and F. London, *Z. Phys.*, 1927, **44**, 455–472.
67 Y. Sugiura, *Z. Phys.*, 1927, **45**, 484–492.
68 G. H. Dieke and J. J. Hopfield, *Phys. Rev.*, 1927, **30**, 400–417.
69 S. C. Wang, *Phys. Rev.*, 1928, **31**, 579–586.
70 O. W. Richardson and P. M. Davidson, *Proc. R. Soc. London, Ser. A*, 1929, **123**, 466–488.
71 N. Rosen, *Phys. Rev.*, 1931, **38**, 2099–2114.
72 H. M. James and A. S. Coolidge, *J. Chem. Phys.*, 1933, **1**, 825–835.
73 H. M. James and A. S. Coolidge, *J. Chem. Phys.*, 1935, **3**, 129–130.
74 H. Beutler, *Z. Phys. Chem. Abt. B*, 1934, **27**, 287–302.
75 H. Beutler, *Z. Phys. Chem. Abt. B*, 1935, **29**, 315–327.
76 W. Kołos and C. C. J. Roothaan, *Rev. Mod. Phys.*, 1960, **32**, 219–232.
77 G. Herzberg and A. Monfils, *J. Mol. Spectrosc.*, 1961, **5**, 482–498.
78 W. Kołos and L. Wolniewicz, *Phys. Lett.*, 1962, **2**, 222–223.
79 W. Kołos and L. Wolniewicz, *Rev. Mod. Phys.*, 1963, **35**, 473–483.
80 W. Kołos and L. Wolniewicz, *J. Chem. Phys.*, 1964, **41**, 3674–3678.
81 L. Wolniewicz, *J. Chem. Phys.*, 1966, **45**, 515–523.
82 B. Jeziorski and W. Kołos, *Chem. Phys. Lett.*, 1969, **3**, 677–678.
83 S. Takezawa, *J. Chem. Phys.*, 1970, **52**, 2575–2590.
84 G. Herzberg, *Phys. Rev. Lett.*, 1969, **23**, 1081–1083.
85 W. C. Stwalley, *Chem. Phys. Lett.*, 1970, **6**, 241–244.
86 P. R. Bunker, *J. Mol. Spectrosc.*, 1972, **42**, 478–494.
87 W. Kołos and L. Wolniewicz, *J. Mol. Spectrosc.*, 1975, **54**, 303–311.
88 D. M. Bishop and L. M. Cheung, *Phys. Rev. A: At., Mol., Opt. Phys.*, 1978, **18**, 1846–1852.
89 L. Wolniewicz, *J. Chem. Phys.*, 1983, **78**, 6173–6181.
90 W. Kołos, K. Szalewicz and H. J. Monkhorst, *J. Chem. Phys.*, 1986, **84**, 3278–3283.
91 C. Schwartz and R. J. Le Roy, *J. Mol. Spectrosc.*, 1987, **121**, 420–439.
92 A. Balakrishnan, V. Smith and B. P. Stoicheff, *Phys. Rev. Lett.*, 1992, **68**, 2149–2152.
93 A. Balakrishnan, V. Smith and B. P. Stoicheff, *Phys. Rev. A: At., Mol., Opt. Phys.*, 1994, **49**, 2460–2469.
94 E. E. Eyler and N. Melikechi, *Phys. Rev. A: At., Mol., Opt. Phys.*, 1993, **48**, R18–R21.
95 W. Kołos and J. Rychlewski, *J. Chem. Phys.*, 1993, **98**, 3960–3967.
96 L. Wolniewicz, *J. Chem. Phys.*, 1995, **103**, 1792–1799.
97 R. E. Moss, *J. Chem. Soc., Faraday Trans.*, 1993, **89**, 3851–3855.
98 R. E. Moss, *J. Phys. B: At., Mol. Opt. Phys.*, 1999, **32**, L89–L91.
99 D. Sprecher, S. Burkhard and F. Merkt, *unpublished results*, the Franck–Condon factors were determined in the adiabatic approximation using the potential energy curves of H_2

from Ref. 60, 61, 62–63 and 62 for the *X*, *EF*, *H* and *O* states, respectively. For higher excited states the potential energy curve of the X^+ state of H_2^+ from Ref. 64 was used.

100 P. Quadrelli, K. Dressler and L. Wolniewicz, *J. Chem. Phys.*, 1990, **93**, 4958–4964.
101 D. Sprecher, Ch. Jungen and F. Merkt, *unpublished results*, the energies of the gerade low-*n* Rydberg states were determined in preliminary MQDT calculations.

This journal is © The Royal Society of Chemistry 2011